Gain Optimization Method of a DQW Superluminescent Diode with Broad Multi-State Emission

C.E. Dimas[1], H.S. Djie[2], B.S. Ooi[3]
Department of Electrical and Computer Engineering, Lehigh University, Bethlehem, Pennsylvania 18015, U.S.A
Presently with: [1]Masdar Institute (UAE), [2] JDS Uniphase (USA), [3] King Abdullah University of Science and Technology (KSA)
Email: [1]cdimas@masdar.ac.ae

***Abstract*-Optimizing gain through systematic methods of varying current injection schemes analytically is significant to maximize experimentally device yield and evaluation. Various techniques are used to calculate the amplified spontaneous emission (ASE) gain for light emitting devices consisting of single-section and multiple-sections of even length. Recently double quantum well (DQW) superluminescent diodes (SLD) have shown a broad multi-state emission due to mutli-electrodes of non-equal lengths and at high non-equal current densities. In this study, we adopt an improved method utilizing an ASE intensity ratio to calibrate a gain curve based on the sum of the measured ASE spectra to efficiently estimate the gain. Although the laser gain for GaAs/AlGaAs material is well studied, the ASE gain of SLD devices has not been systematically studied particular to further explain the multiple-state emission observed in fabricated devices. In addition a unique gain estimate was achieved where the excited state gain clamps prior to the ground state due to approaching saturation levels. In our results, high current densities in long sectioned active regions achieved sufficient un-truncated gain that show evidence of excited state emission has been observed.**

I. INTRODUCTION

Superlumienscent diodes (SLDs) have a great number of applications in interferometric sensing such as optical coherent tomography and optical gyroscopes due to the required broad spectral bandwidth for high axial resolution [1]. Techniques to measure the modal gain is significant in revealing the origin of the bandwidth and output power as well as calculating other device and material properties for device optimization.

SLDs operate at the superlinear, amplified spontaneous emission (ASE) regime of the luminescence versus current (L-I) curve. The modal gain is defined as the fractional increase of the intensity of an optical mode per unit distance of propagation. Typically the modal gain in SLDs is at least two times higher than threshold modal gain in laser diodes [2], since SLDs have device features to suppress lasing.

Comparing published ASE measurement techniques summarized in Table I, it is evident that certain approaches require a set of conditions, such as equal segments, equal current density, and a particular number of active sections. Our multi-electrode SLD design (previously detailed in [3]) consists of two active ridge sections (D_1, D_2) butt-coupled to a slab waveguide photon absorber. The D_2 (middle) section is a fixed length and the D_1 (by emitter facet) section is adjustable in length up to 1 mm. The D_1 section can therefore support greater current density than the D_2 section. In addition, long cavity lengths and high current density can lead to saturation, which can therefore impede gain measurements. Saturation occurs when the ASE intensity shows the depleted excited state (ES) population reducing the ES gain as the signal intensity builds up along the amplification axis [4,5]. Therefore, the longer the cavity, the more susceptible a device is to approaching saturation at high injection currents.

Although there has been recent work on multiple-section ASE gain calculations when characterizing quantum well (QW) lasers [6-8], the ASE gain of QW SLDs has not been quantified. In addition, no other work has shown multiple state gain in symmetric QW based material structures. Oster *et al.* [6] implemented the segmented device gain technique from Blood *et al.* [8], which uses the ratio of measured ASE spectra. The material characterized was an InGaAsP/AlGaAs multiple-section laser device emitting at 800 nm. The maximum injected current density reported was 1.6 kA/cm^2 and the active region consists of two QWs which were 6 nm thick. The gain curves confirmed the emission is only from the ground state energy level. Since our GaAs/AlGaAs wells are 10 nm thick each, we can achieve higher current densities which in turn enable an ES gain. Quantifying gain can demonstrate ES emission as well as the role of saturation in our device.

TABLE I
Comparison of ASE gain approximation methods

Method	Active Sections	Basis	J_{D1} … J_{Dn}	L_{D1} … L_{Dn}	Other Factors
Hakki, Paoli [7]	1	FP modes	-	-	Limited current density
Lin [9] *Two-section technique*	2	Sum of ASE	Non-uniform	Not equal	ASE from two facets
Blood [6] *Segmented contact method*	2	Ratio of ASE	Uniform	Not equal	Fit to get gain
Blood [6] *Segmented contact method*	2	Ratio of ASE	Uniform	Equal	
Lester [12] *Alternative segmented contact method*	3	Ratio of ASE	Uniform	Equal	Factors in current leakage

J_{D1} is the current density in section D_1
L_{D1} is the length in section D_1

II. Results and Discussion

A. Single-Section Device

Several single section modal gain approximations have been formulated. The Hakki Paoli method for instance examines the Fabry-Perot (FP) modulation of the ASE of a laser device at subthreshold current densities using the following equation [9].

$$G = \frac{1}{L}\ln\left(\frac{\sqrt{I_{\max}}+\sqrt{I_{\min}}}{\sqrt{I_{\max}}-\sqrt{I_{\min}}}\right)+\frac{1}{L}\ln(R), \quad (1)$$

where I_{max} refers to a peak of a FP mode, I_{min} refers to a valley of a FP mode, L is the active length, R is the facet reflectance. By fitting the measured ASE spectra at various current densities to a series of Lorentzian functions, the minimum and maximum points are extracted to generate the modal gain. The limitation of this method is the maximum current density and OSA resolution. The maximum current density under threshold is less than the current density achievable in SLDs which have absorbing sections and low reflectance facets. In addition, since the cavity length is inversely proportional to the period of the FP modulation, the cavity length must be small enough for the OSA not to undersample the FP modes of the wide the spectrum. Modal gain calculated using the Hakki-Paoli method for a GaAs/AlGaAs single ridge section device is shown in Fig. 1. As seen from the data, the gain increases with current injection density up to 3.42 kA/cm^2 with a peak at 862 nm. Note that above the threshold current, a single lasing peak at 865 nm is observed for the corresponding cavity length of 0.03 cm. This single section gain approach falls short of easily demonstrating an ES gain. The following gain approximation methods discussed involve having longer sections, thus enabling higher current densities.

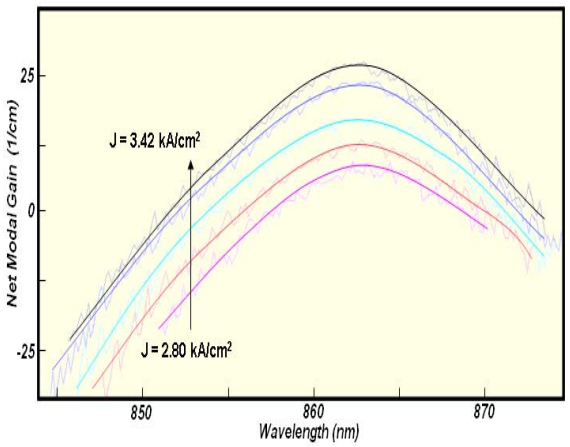

Fig. 1. Hakki Paoli Gain approximation of a GaAs/AlGaAs DQW single section ridge device with a cavity length of 0.03 cm at varying current densities.

A gain calculation method based on the sum of ASE spectra is derived and implemented. The semiconductor optical amplifier (SOA) equation is as follows [10]:

$$\frac{dP}{dL} = GP, \quad (2)$$

where P is optical power at distance L from the input at $L=0$, and G is net modal gain. For a constant gain, a solution to Equation (2) is the following [10].

$$P(L) = P_{in}e^{GL}, \quad (3)$$

where $P(L)$ refers to optical power at distance L, and P_{in} is the input optical power at L=0. The term $exp(GL)$ is also referred to as the amplified gain. From Equation (3), Lin *et al.* [11] applied the following set of equations to calculate the optical gain from a two-section SOA device:

$$I_{D1}(\lambda, J_{D1}, J_{D2}) = CI_{D2}(\lambda, 0, J_{D2})e^{G(\lambda, J_{D1})L_{D1}} + I_{D1}(\lambda, J_{D1}, 0), \quad (4)$$

$$G(\lambda, J_{D1}) = \left(\frac{1}{L_{D1}}\right)\ln\left(\frac{I_{D1}(\lambda, J_{D1}, J_{D2}) - I_{D1}(\lambda, J_{D1}, 0)}{CI_{D2}(\lambda, 0, J_{D2})}\right), \quad (5)$$

where $I_{D1}(\lambda, J_{D1}, J_{D2})$ corresponds to the ASE intensity from facet D_1 when the current density of section D_1 equals J_{D1} and the current density of section D_2 equals J_{D2}. C is a coupling factor quantifying the coupling variation in measurement when coupling into each facet. As shown, the net modal gain, $G(\lambda, J_{D1})$ is not dependent on J_{D2}, which therefore can be of any value.

The benefit of this ASE sum approach is that it does not depend on sections of equal length nor equal current densities. This is especially beneficial when one section is much shorter, as is the case in our multiple-section design.

Fig. 2(a) shows the measured spectra from each facet while injecting each section individually as well as injecting both sections simultaneously. Using Equation (5), the gain from each section of a two-section GaAs/AlGaAs ridge device is examined in Fig. 2(b). Applying this two-section two-facet method to our straight ridge device limits our current density in order to maintain sub-threshold conditions. Lin *et al.,* on the other hand, applied this gain method to a set of tilted ridge SOAs and therefore achieved high current density [9]. Due to the limitation in our current injection, the gain spectrum only corresponds to the ground state. In addition, saturation in the longer section is observed during wavelengths, where $I_{D2}(\lambda, J_{D1}, J_{D2})$ is less than $I_{D2}(\lambda, 0, J_{D2})$ forcing gain to be an imaginary and therefore invalid value. Even though the D_2 section is injected at higher current density than D_1, saturation does not occur because it is a shorter section. One more important observation is the similar gain shape for the similar injection current densities. The gain for the longer section, D_1, seems truncated. In summary, a higher current density with less saturation effects is needed as well as a way to derive *C*. Although the section lengths and current densities do not have to be equal, the coupling factor *C* has to be calculated to yield gain in real units.

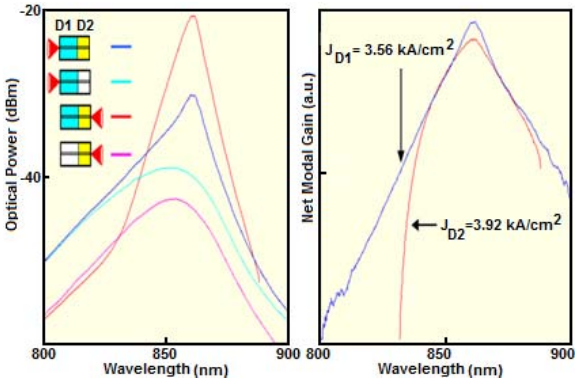

Fig. 2. (a) The spectrum and (b) the corresponding uncalibrated net modal gains of a two section GaAs/AlGaAs ridge device. The inset in (a) illustrates the emitting facet that corresponds to each spectrum.

C. Multiple-section Device, Equal Current Density

The optical gain, the differential change in the ASE intensity with transmission length, *L*, and the pure spontaneous emission, P_s, can be related by the following equation [12]:

$$\frac{dI}{dL} = GI + P_S, \tag{6}$$

Using the boundary condition of $I=0$ at $x=0$, the single pass emission equation is derived [13].

$$I_L(\lambda, J) = \frac{P_S(\lambda, J)}{G(\lambda, J)}[e^{G(\lambda,J)L} - 1], \tag{7}$$

where I_L corresponds to ASE intensity with active length, *L*, P_s is the uncalibrated pure unamplified spectrum. Assuming uniform current injection and that gain is independent of length, Blood *et al.* [8] used a ratio of ASE spectra to calculate gain in a multiple-section device with the following equation.

$$r_x = \frac{I_{xL}(\lambda, J)}{I_L(\lambda, J)} = \frac{e^{G(\lambda,J)xL} - 1}{e^{G(\lambda,J)L} - 1}, \tag{8}$$

where r_x is the ratio of ASE intensities, and *x* is the scalar factor between the lengths. In order to match our previous convention of the subscript of *I* pertaining to the facet, the equation is re-written in the following manner for consistency:

$$r_x = \frac{I_{D1}(\lambda, J, J)}{I_{D1}(\lambda, J, 0)} = \frac{e^{G(\lambda,J,J)*(xL_{D1})} - 1}{e^{G(\lambda,J,0)*L_{D1}} - 1}, \tag{9}$$

where $I_{D1}(\lambda,J,J)$, corresponds to ASE intensity from facet D_1, where $J_{D1} = J_{D2} = J$. The corresponding lengths are L_1 and L_2, and xL_{D1} equals $L_{D1}+L_{D2}$. In addition, a few conditions are necessary to implement the above set of equations given uniform density and length independence assumptions: 1) lasing is fully suppressed by the PA, 2) spatial filtering is accomplished with a tapered single mode fiber, 3) single mode emission is accomplished by having a 4 μm ridge waveguide. Although the analytical solution to gain exists for equal sectioned devices in a simple form [14], the estimate is dependent on fixed non-optimal device lengths and long length intervals making measurements more vulnerable to saturation [7].

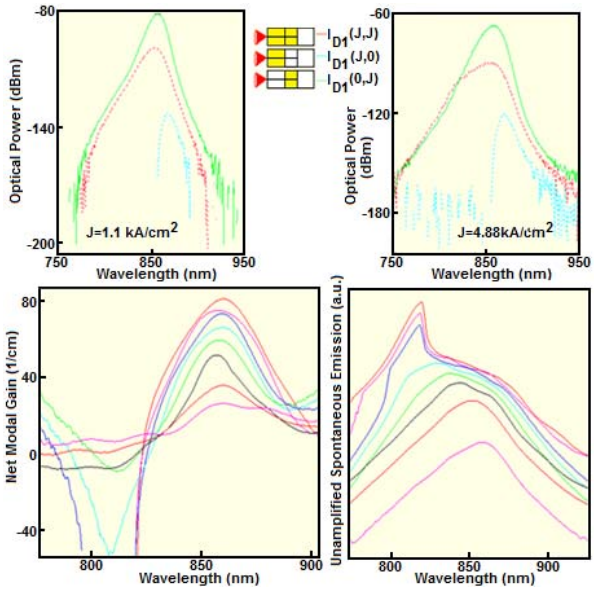

Fig. 3. The spectrum (a),(b), gain (c), and uncalibrated spontaneous emission (d) of a 3-section SLD at equal current densities ranging from 1.1 kA/cm^2 to 4.88 kA/cm^2. The insets of (a),(b) show the spectrum were taken by pumping both sections, as well as D_1 and D_2 individually.

Fig. 3 demonstrates the spectrum of pumping various sections of a GaAs/AlGaAs SLD with equal current densities

as well as the corresponding gain and spontaneous emission estimates. As evident in Equation (9), r_x cannot be below 1, otherwise absorption is greater than gain. The ASE spectra ratio, r_x, varies between 0 and 1 for the wavelengths (810 nm - 830 nm) because $I_{D1}(J,0)$ is greater than $I_{D1}(J,J)$. Therefore saturation impedes evidence of an ES gain. With a smaller I_{D2} than I_{D1}, less saturation effects may occur. Therefore, using a gain method allowing unequal current density is necessary.

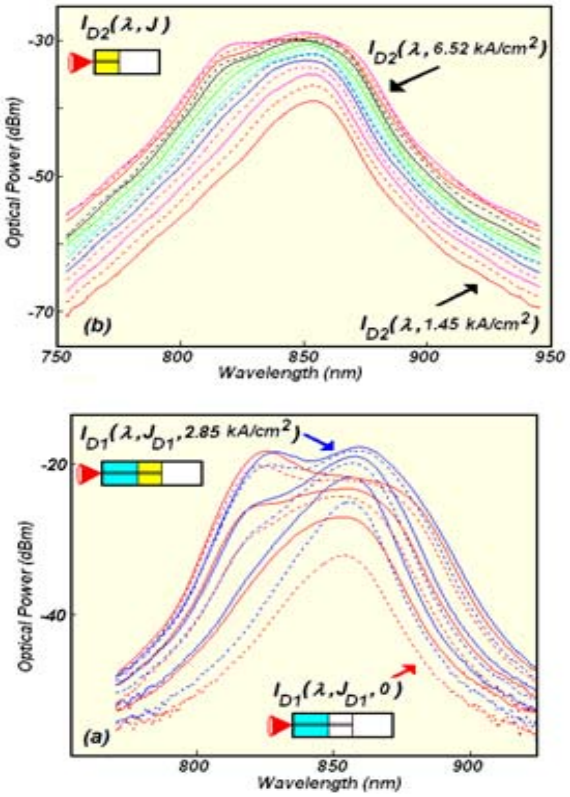

Fig. 4. Spectrum by pumping various regions: (a) ASE intensity from the D_2 facet at various D_2 current densities (1.45 – 6.52 kA/cm^2) (b) Spectrum of pumping of both sections (blue) and front section (red) for a three-section Gas/AlGaAs SLD with current densities ranging from 0 kA/cm^2 to 10.48 kA/cm^2 for D_1 and fixed at 2.85 kA/cm^2 for D_2.

D. Multiple-section Device, Unequal Current Density

In this section, we devise a technique to measure the gain of our two-section ridge SLD with integrated PA devices which have different sectioned lengths. First the ASE ratio and sum approach (Equation (5), Equation (9)) are used to solve for the gain while pumping the same current density in each section (D_1, D_2). As discussed, the ASE ratio yields gain in real values, while the sum approach yields results in relative values when setting C (from Equation (5)) to unity. Therefore by setting these two gains to one another, C can be found.

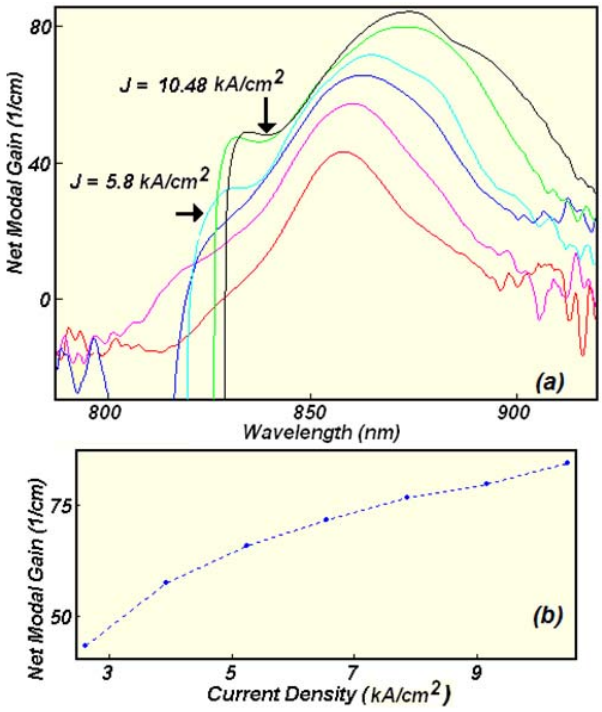

Fig. 5. Calculated net modal gain increases with increasing current densities. At J = 5.8 kA/cm^2, the gain for the ES begins to be prominent.

In our approach, $I_{D2}(\lambda, 0, J_{D2})$ from Equations 4 and 5, now pertains to the spectra of a 1-section D_2 ridge with integrated PA SLD rather than emission from the same device at the opposite facet. In other words, the D_1 section has been cleaved off for spectra requiring a D_2 facet emission, as shown in Fig. 4(a) inset. $I_{D1}(\lambda,0,J_{D2})$ is measured while J varies from 1.45 to thermal roll off which is 6.52 kA/cm^2. Since all of our multiple-section devices have a fixed 0.035 cm D_2 section, the $I_{D2}(\lambda,0,J)$ measurements will serve to measure the gain for any length and current density of D_1 by using Equation (5). The ASE sum equations are then applied to our multiple-section device. As shown in Fig. 4(b), $I_{D1}(\lambda, J_{D1}, 0)$, *and* $I_{D1}(\lambda,J_{D2},$ 2.85 kA/cm^2) are measured for values of J_{D1} up to 10.48 kA/cm^2. J_{D2} was chosen because it yields a clean spectra $I_{D1}(\lambda,0,$ 2.85 kA/cm^2). By examining the gain emission shown in Fig. 5, one can observe a distinct gain hump corresponding to the ES emission of the spectra, followed by a truncated gain due to saturation. If J_{D2} had been set to equal J_{D1}, saturation and thermal roll-off would have impeded any evidence of the ES gain. No gain curve previously for symmetric QWs had previously been observed. In addition, the maximum gain with increasing current density is approaching a flattening point. This new multiple-section, unequal current density approach is a simple straight forward way to calculate the net modal gain.

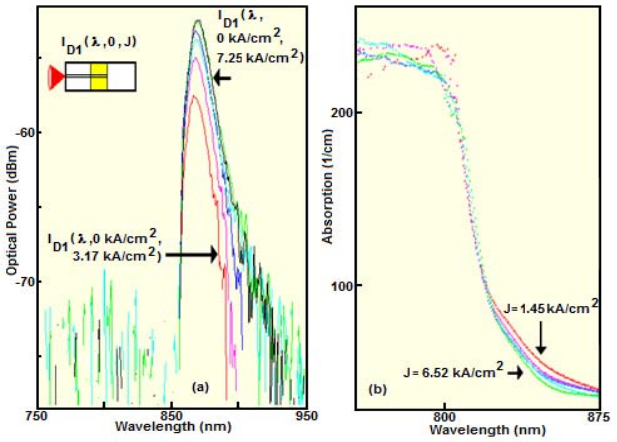

Fig. 5. Spectrum by pumping various regions: (a) ASE intensity from the D1 facet at various D2 current densities while D1 is unpumped, (b) Absorption at various current densities.

E. Loss Measurements

Loss measurements can also be measured from multisection devices. By measuring two spectra: $I_{D2}(\lambda, 0, J_{D2})$ - Fig. 4(b) and $I_{D1}(\lambda, 0, J_{D2})$ - Fig. 6(a), the following equations can be used to yield the corresponding absorption curve [15]:

$$I_{D1}(\lambda,0,J_{D2}) = I_{D2}(\lambda,0,J_{D2})e^{-\alpha L_{D1}}, \tag{10}$$

$$\alpha = \frac{-1}{L_{D1}} \ln\left(\frac{I_{D1}(\lambda,0,J_{D2})}{I_{D2}(\lambda,0,J_{D2})}\right), \tag{11}$$

where α is the optical loss co-efficient of the waveguide. In general this equation is used for segmented devices of equal length. In the equal section case, $I_{D2}(\lambda, 0, J_{D2}) = I_{D1}(\lambda, J_{D1},0)$, which therefore only involves one fiber coupling setup. However, since our D_1 section is not fixed, the measurement of $I_{D2}(\lambda, 0, J_{D2})$ which is necessary for our new gain approximation, is also useful for loss measurements. As the D1 section absorbs all but the ground state emission from the mid section emission, Fig. 6(b) clearly illustrates the absorption edge at 860 nm. In addition, we observe that αi is ~ 30 cm^{-1} as the absorption curves converge to this value.

III. Summary

Various techniques were examined to explain our segmented multiple-state GaAs/AlGaAs SLD emission. A new technique was devised to measure gain for an unequal segmented and unequally pumped two-section ridge SLD. In addition a unique gain estimate was achieved where the ES state gain clamps prior to the GS due to approaching saturation levels. High current densities in long sectioned active regions achieved sufficient un-truncated gain to show evidence of ES excitation.

Acknowledgment

This work was supported in part by the National Science Foundation (NSF) under Grant No. 0725647, US Army Research Laboratory, Commonwealth of Pennsylvania, Department of Community and Economic Development.

References

[1] H.D. Huang, E.A. Swanson, C.P. Lin, J.S. Shuman, W.G. Stinson, W. Chang, M.R. Hee, T. Flotte, K. Gregory, C.A. Puliafito, and J.G. Fujimoto, "*Optical Coherence Tomography*," Science, Vol. 254, pp. 1178, 1991.

[2] V. Shidlovski, "*Superluminescent Diodes.Short overview of device operation principles and performance parameters*," Superlum White Paper, 2004.

[3] C.E. Dimas, H.S. Djie, B.S. Ooi, "Superluminescent Diodes using Quantum Dot Superlattice," Journal of Crystal Growth, Vol. 288, No. 1, pp. 153-156, 2006.

[4] L. Dal Negro, P. Bettotti, M. Cazzanelli, D. Pacifici, L. Pavesi, "*Applicability conditions and experimental analysis of the variable stripe length method for gain measurements*," Optics communications, Vol. 229, No. 1-6, pp. 337-348, 2004.

[5] Y. Dankner, "*Optical gain and saturation of photoexcited type-II superlattice*," Solid State Comm., Vol. 93, No. 8, pp. 707-712, 1995.

[6] A. Oster, F. Bugge, G. Erbert, I. Rechenberg, A. Thies, H. Wenzel, "*Gain spectra measurement of strained and strain compensated InGaAsP/AlGaAs laser structures for λ~800 nm using a new variable stripe length method*," Semiconductor Laser Conference, Vol., No. 4-8, pp. 169 - 170, 1998.

[7] C. Lange, M. Schwalm, S. Chatterjee, W.W. Rühle, N.C. Gerhardt, S.R. Johnson, J.-B. Wang, Y.-H. Zhang, Y.-H, "*The variable stripe-length method revisited: Improved analysis*," Appl. Phys. Lett., Vol. 91, No. 19, pp. 191107-10, 2007.

[8] P. Blood, G.M. Lewis, P.M. Smowton, H. Summers, J. Thomson, J. Lutti, "*Characterization of semiconductor laser gain media by the segmented contact method,"* Sel. Top. Quant. Elect., Vol. 9, No. 5, pp. 1275 - 1282, 2003.

[9] B.W. Hakki, T.L. Paoli, "*Gain spectra in GaAs double-heterostructure injection lasers*," J. App. Phys., Vol. 46, pp. 1299-1306, 1975.

[10] N. Dutta and Q. Wang, *Semiconductor Optical Amplifiers*, World Scientific, New Jersey, 2006

[11] C.-H. Wu; Y.-S. Su; C.-F. Lin, "*Measurement of broadband gain spectrum of semiconductor optical amplifiers using a two-section technique*," Lasers and Electro-Optics Conference, Vol. 1, No. 16-21, pp. 3-6, 2004.

[12] J. T. Verdeyen, *Laser Electronics*. Englewood Cliffs, NJ: Prentice-Hallt, 1995.

[13] A. Yariv, *Quantum Electronics*, 2nd Edition, Wiley & Sons, New York, 1974.

[14] Y.-C. Xin, L. Yan, A. Martinez,T.J. Rotter,S. Hui, Z. Lei, A.L. Gray, S. Luong, K. Sun, Z. Zou, J. Zilko, P.M. Varangis, L.F. Lester, "*Optical gain and absorption of quantum dots measured using an alternative segmented contact method*," Quant. Elect., Vol. 42, No. 7, pp. 725 - 732, 2006.

[15] H.D. Summers, P.M. Smowton, P. Blood, M. Dineen, R.M. Perks, D.P Bour, M. Kneissel, "*Spatially and spectrally resolved measurement of optical loss in InGaN laser structures*," J. Crystal Growth, Vol. 230, No. 3-4, pp. 517-521, 2001.